Journal of Structural Geology, Vol. 12, No. 4, pp. 419 to 430, 1990
Printed in Great Britain

0191-8141/90 $03.00+0.00

State of strain in mylonites from the western Blue Ridge province, southern Appalachians: the role of volume loss

KIERAN O'HARA

Department of Geological Sciences, University of Kentucky, Lexington, KY 40506, U.S.A.

(*Received* 20 *February* 1989; *accepted in revised form* 10 *December* 1989)

Abstract—This study examines the state of finite strain in quartzo-feldspathic mylonites from two localities in the western Blue Ridge province of the southern Appalachians. Mineral shape fabric and whole-rock chemical and modal data suggest that the mylonites deformed by inhomogeneous shortening normal to the foliation and progressive shear parallel to the foliation. The deformation involved substantial bulk-rock volume loss. Strain was partitioned between solution transfer processes in feldspar and dislocation creep processes in quartz and micas at temperatures of between 300 and 450°C. Initially feldspars underwent grain-size reduction by cataclasis but at advanced stages of mylonitization alkali feldspar grains display subrounded oblate shapes ($0 < k < 0.5$) which are attributed to dissolution processes normal to the foliation. Quartz deformed by crystal-plastic processes and quartz grains and ribbons display a range of k values ($0.2 < k < 0.9$) reflecting heterogeneous deformation. Whole-rock mylonite samples are enriched by a factor of 3 relative to their gneissic protolith in 'immobile' trace elements such as Ti, Zr, Y, P and V, and the REE which is attributed to the concentration of residual phases such as zircon, apatite, epidote and ilmenite observed in the mylonites. The trace element enrichments are interpreted as due to large (>60%) bulk volume loss. Density changes were minor. On the basis of feldspar grain shapes and modal and whole-rock chemical data, volume loss was largely accommodated by fluid infiltration and incongruent dissolution of alkali feldspar (producing muscovite) and involved the loss of alkalis and silica to the fluid phase. The mylonites may have nucleated as solution zones which subsequently underwent strain softening and displacement parallel to the zone boundaries.

INTRODUCTION

EVIDENCE for non-coaxial strain accumulation in ductile shear zones (e.g. Berthé *et al.* 1979) together with theoretical considerations of ideal shear zones (Ramsay & Graham 1970) suggest that many shear zones can be modeled on the basis of heterogeneous simple shear (e.g. Escher *et al.* 1975, Simpson 1983). Detailed strain analyses of mylonites from shear zones, however, commonly show flattening types of finite strain that deviate from a plane strain geometry (Coward 1976, Choukroune & Gapais 1983, Mawer 1983). Such strains may be better modeled on the basis of shear bands which have a component of shortening normal to the shear-zone boundaries (e.g. Cobbold 1977). Bell (1981) suggested bulk heterogeneous shortening as a model for deformation in rock which deformed along conjugate shear zones (see also Choukroune & Gapais 1983, Boyer & Mitra 1988) and that space problems associated with bulk shortening can be resolved if volume change is involved. Since volume loss can be incorrectly attributed to true flattening (Ramsay & Wood 1973), and volume changes in shear zones can be difficult to quantify, volume loss associated with heterogeneous flattening in shear zones may be more important than commonly recognized. This may be particularly true of retrograde shear zones in crystalline terranes where evidence for fluid infiltration and feldspar dissolution is found (e.g. Mitra 1978, Boyer & Mitra 1988, Janecke & Evans 1988, O'Hara 1988).

Recent geochemical studies of greenschist-facies mylonites from the Rector Branch Thrust, North Carolina, and the Fries Thrust, Virginia, in the southern Appalachians indicate that 'immobile' element enrichments in the mylonites are due to large (~60%) volume losses (O'Hara 1988, O'Hara & Blackburn 1989). In order to better characterize the state of finite strain in these rocks this study presents microstructural observations, estimates of dilational strains, and mineral shape fabric data for quartz and feldspar. The combined observations indicate that the mylonites from both localities have undergone heterogeneous shortening normal to the foliation (involving volume loss) and a component of noncoaxial shear parallel to the foliation. In general, volume loss in mylonites has important implications for the state of strain in ductile shear zones, the application of strain techniques for estimating displacements across these zones and for the role of mass transfer processes during deformation.

MYLONITES

Tectonic setting

Mylonites from two similar thrust settings were studied; the Fries Thrust in Virginia and the Rector Branch Thrust along strike in North Carolina (Figs. 1a & b). The mylonites are in structurally similar settings insofar as both thrusts juxtapose Grenvillian crystalline gneisses of the Blue Ridge in the hanging wall with weakly meta-

morphosed late Precambrian to Lower Paleozoic metasediments in the footwall.

The Fries Thrust is represented by a wide zone of mylonitized granitic gneiss (1–2 km wide in map view; 800 m in true thickness) which juxtaposes (Grenvillian ?) paragneisses (Ashe Formation) in the southeast against the Cambrian-aged Unicoi Formation and the underlying Grayson Gneiss to the northwest (Stose & Stose 1957) (Fig. 1a). The Rector Branch Thrust lies along strike southwest of Fries in North Carolina along the southern margin of the Hot Springs window. This is an eyelid window indicating that the thrust sheets which bound the southern and northern margins are separate and distinct (Oriel 1951). The Rector Branch Thrust is also marked by a wide zone of mylonitic rocks derived from the overlying gneisses and it juxtaposes Grenvillian gneiss (Max Patch Granite) in the southeast with late Precambrian Snowbird Group metasediments to the north (Oriel 1951) (Fig. 1b). The mylonites from both locations are mineralogically similar (Table 1).

Petrography

The protolith rocks are medium-grained (2–3 mm) gneisses, granitic to granodioritic in composition (Tables 1 and 2), and typically contain quartz, alkali

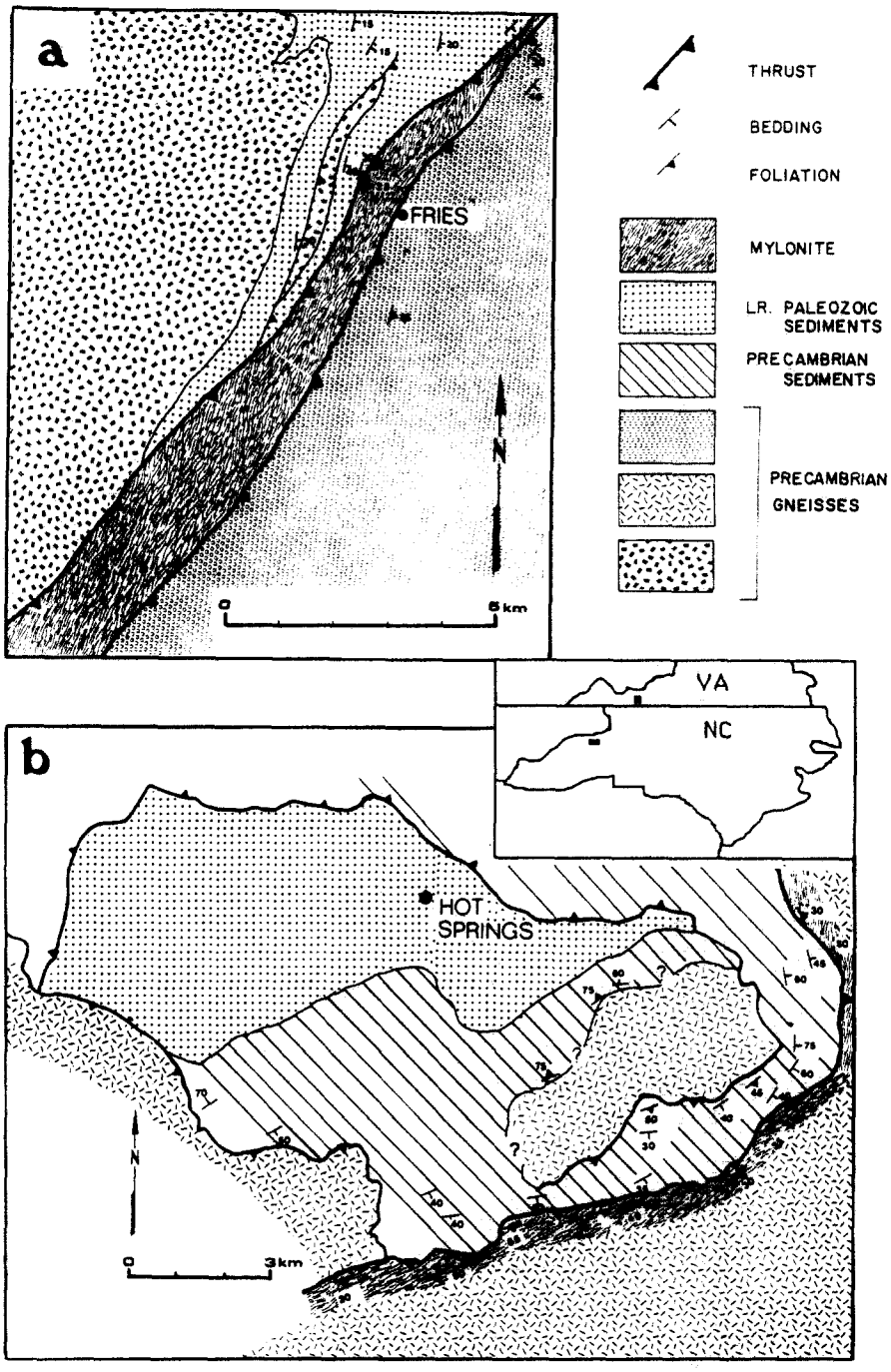

Fig. 1. Inset map shows the locations of the two areas. (a) Generalized geologic map of the Fries Thrust in the vicinity of Fries, Virginia (VA), after Stose & Stose (1957). (b) Generalized geologic map of the Hot Springs window, North Carolina (NC), modified from Oriel (1951). The Rector Branch Thrust is marked by a wide zone of mylonite along the southern margin of the window.

feldspar (microcline and perthitic orthoclase), albite-twinned plagioclase, biotite and accessory zircon, epidote and apatite (Fig. 2a). In the field a moderately well developed regional foliation is subparallel to the mylonitic foliation, and is defined in thin section by elongated non-recrystallized undulose quartz grains (Fig. 2a) and biotite grains. Alkali feldspar in the gneisses typically displays minor hydrothermal alteration along fractures (Fig. 2a). In the protomylonites feldspars behave brittlely and typically display extension and shear fractures which result in production of angular and elongated fragments (Fig. 2b). These fractures commonly contain secondary chlorite, epidote or quartz.

Table 1. Modal data (%) for gneisses and mylonites*

	Fries		Hot Springs	
	Gneisses	Mylonites	Gneisses	Mylonites
	N		*N*	
	1	3	5	3
Quartz	32	32	35	29
K-feldspar	49	12	36	18
Muscovite	4	25	13	25
Plagioclase	1	2	6	8
Biotite	1	1	3	9
Chlorite	8	22	3	3
Epidote	1	1	2	2
Opaques	1	3	1	2
Zircon	1	1	1	1
Density (g cm^{-3})†	2.6	2.75	2.7	2.8

*500 points per sample.
†Bulk density based on modal composition using representative mineral densities.

Plagioclase is sometimes partly altered to white mica and epidote or zoisite. In hand-specimen these alteration effects are indicated by a green coloration along fractures.

In mylonitic samples quartz is usually present as elongate monocrystalline and polycrystalline 'ribbons' with aspect ratios as high as 20:1 in sections parallel to the lineation and normal to the foliation (Fig. 2c). This is in contrast to feldspar which behaves more rigidly and initially undergoes grain-size reduction by brittle processes. Both alkali and plagioclase feldspars are commonly rimmed by selvages of muscovite (Fig. 2d) suggesting a reaction relationship between the two minerals. In sections normal to the foliation these feldspar clasts are commonly subrounded to rounded and elliptical in shape (Fig. 2d). The foliation which wraps around the clasts commonly contains concentrations of high relief phases such as zoisite, apatite, zircon, pyrite and ilmenite (Figs. 2d and 3a). The inhomogeneous distribution of these minerals makes reliable estimation of their abundance difficult. Evidence for non-coaxial strain includes asymmetric tails of recrystallized quartz and muscovite around feldspar clasts (sigma type, Passchier & Simpson 1986) and occasional asymmetric mica fish (Fig. 3b). In general, however, feldspars display orthorhombic symmetry with respect to the foliation (Figs. 2d and 3a). Oblique healed transgranular fractures are commonly present in the mylonites (Fig. 2c) which often contain small quartz hosted liquid–vapor fluid inclusions. Freezing stage measurements indicate the fluids are moderately saline (>15 wt % NaCl equiv.).

Comparison of the mylonites with the protolith

Table 2. Whole-rock chemical analyses of gneisses and mylonites

	Fries Thrust				Rector Branch Thrust (O'Hara 1988)			
	Gneisses		Mylonites		Gneisses		Mylonites	
	Mean (*N* = 3)	S.D.	Mean (*N* = 5)	S.D.	Mean (*N* = 5)	S.D.	Mean (*N* = 9)	S.D.
SiO_2	76.21	2.9	66.3	2.07	70.45	2.15	62.90	1.5
TiO_2	0.22	0.03	0.72	0.23	0.28	0.12	1.03	0.2
Al_2O_3	12.36	1.63	15.23	0.61	14.17	0.68	15.0	0.59
Fe_2O_3	1.84	0.28	4.79	1.69	2.42	0.75	6.43	0.69
MnO	0.03	0.01	1.15	0.47	0.04	0.03	0.11	0.02
MgO	0.33	0.05	1.13	0.66	0.68	0.35	1.30	0.27
CaO	0.68	0.11	5.20	1.82	1.90	0.53	2.35	0.09
Na_2O	4.15	0.94	3.26	1.38	3.15	0.22	3.68	0.56
K_2O	3.03	1.25	1.50	0.28	4.76	0.37	4.08	0.60
P_2O_5	0.04	0.02	0.2	0.06	0.09	0.04	0.58	0.08
LOI	1.01	0.26	1.50	0.28	0.70	0.34	1.18	0.29
Rb	38	41	53	27	121	23	111	19
Sr	157	107	190	73	373	60	414	171
Y	3	1	16	9	9	6	46	11
Zr	123	23	261	122	140	79	486	63
V	25	14	53	10	32	12	64	20
Ni	4	1	7	4	7	3	6	1
Cr	45	9	47	6	42	11	35	20

Analysis by X-ray fluorescence spectrometry on fused pellets; analyst: S. A. Mertzman, Franklin and Marshall College, Pennsylvania.

gneisses indicates that the major modal mineralogical changes involved during deformation are a decrease in feldspar (from 40–50% in the protolith to 10–20% in the mylonites) and a concomitant increase in white mica (from 5–10% to 25%). Other major phyllosilicates present are chlorite and biotite (Table 1). The higher FeO and MgO concentrations in the mylonites (Table 2) probably reflect the higher modal abundance of these ferromagnesian micas in the mylonites (Table 1). Assemblages of quartz, muscovite, and chlorite and epidote, plagioclase and chlorite, in which quartz is syntectonically recrystallized and the phyllosilicates are parallel to the foliation, indicate greenschist-grade conditions prevailed during deformation. A sheared assemblage consisting of stilpnomelane–epidote–quartz (Fig. 3b) is present at one locality, which together with biotite in the same section, suggests a temperature of less than about 450°C (Winkler 1974, p. 208).

Deformation mechanisms

The lack of substantial recrystallization of feldspar suggests that it did not attain its rounded shape by crystal-plastic processes and this is in substantial agreement with the temperature estimate above since crystal-plastic mechanisms in feldspar are apparently only important above about 450°C (Tullis 1983). The oval shape of the feldspar grains (Figs. 2d and 3a) suggests that cataclasis is not solely responsible for their shapes. On the other hand, the concentration of inert phases around feldspar grains is consistent with pressure solution normal to the foliation. Pressure solution is an important deformation mechanism in silicates at temperatures too low for crystal-plastic mechanisms to operate (e.g. Rutter 1983). Such dissolution may have taken place either by grain-boundary diffusion or by solution in the presence of an advecting fluid (i.e. diffusion transfer as opposed to solution transfer). The large volume losses inferred to have occurred in these rocks (see below) suggests the latter case is more likely (cf. however, Bell & Cuff 1989). Although cataclasis cannot account for the rounded shapes of feldspars, its role in allowing access of fluid during dilatancy (e.g. Fig. 2b) is thought to be crucial in permitting a change to ductile deformation mechanisms (Segall & Simpson 1986, O'Hara 1988).

Quartz deformed by crystal-plastic mechanisms in all the rocks examined. It has either undergone syntectonic recrystallization to form a mosaic of finer, essentially strain-free grains or deformed plastically to produce elongate monocrystalline ribbons (Fig. 2c). These microstructures place a minimum temperature on the deformation since crystal-plastic mechanisms in quartz become important above about 300°C (e.g. Voll 1976). The above considerations suggest that deformation took place between 300 and 450°C. Because the mylonites from both localities have similar macroscopic and microscopic structures and they come from similar tectonic environments they are treated as a single group for the purposes of strain analysis.

STRAIN ANALYSIS

Measurements

Strain in the mylonites is heterogeneous on the outcrop and thin section scales as indicated by a foliation which commonly anastomoses around less deformed gneissic pods in outcrop and also around feldspar clasts at the thin section scale (Fig. 2d). In hand-specimen all the mylonites studied are characterized by a strong foliation defined by quartz ribbons and also by alternating laminations consisting of phyllosilicate-rich layers (chlorite, muscovite and biotite) and quartzofeldspathic layers (Fig. 2c). In hand-specimen a lineation is not always visible but, with the exception of two samples from Fries, thin sections parallel to the foliation reveal a moderate to strong lineation. Thin sections were cut parallel to the foliation (XY), normal to the foliation and lineation (YZ), and normal to the foliation and parallel to the lineation (XZ).

In XY sections the lineation is defined by elongate quartz grains (Fig. 3c), aligned aggregates of phyllosilicates and/or boudinaged apatite grains. Brittlely deformed apatite grains display extension in the X direction but grains parallel to the Y direction show no extension (Fig. 3d). Additional evidence for extension in the X direction includes pulled-apart feldspar fragments elongated parallel to the lineation and extensional quartz or calcite veins normal to the lineation. Similar features indicating extension in the Y direction are not observed suggesting that deformation involved plane strain.

In an effort to examine the state of strain in these rocks in more detail a shape fabric analysis of quartz and feldspar was undertaken. The shapes of both quartz and feldspar grains were measured in nine samples on orthogonal thin sections cut normal and parallel to the foliation and lineation. The long and short axes of approximately 20 quartz and feldspar grains per section were measured (using a digital filar eyepiece attached to a petrographic microscope) and mean aspect ratios for each section were calculated (Table 3). The results are plotted on a logarithmic Flinn diagram (Fig. 4). Quartz from a protolith gneiss (Fig. 2a) displays a flattened fabric (open circle, Fig. 4). Quartz in mylonitic samples from the Rector Branch Thrust show k values ranging from 0.34 to 0.9. Two samples from the Fries Thrust, which in XY sections contain no lineation, display quartz k values of 0.21. Feldspar on the other hand, with the exception of the protolith gneiss (open triangle, Fig. 4) displays flattened strains with k values of between 0 and 0.5.

Errors

Several sources of error are present in the strain analysis above. Not all samples or all grains in a given sample were suitable for strain determination. In the case of quartz this was largely due to recrystallization of grains into a mosaic of subequant finer grains. In the

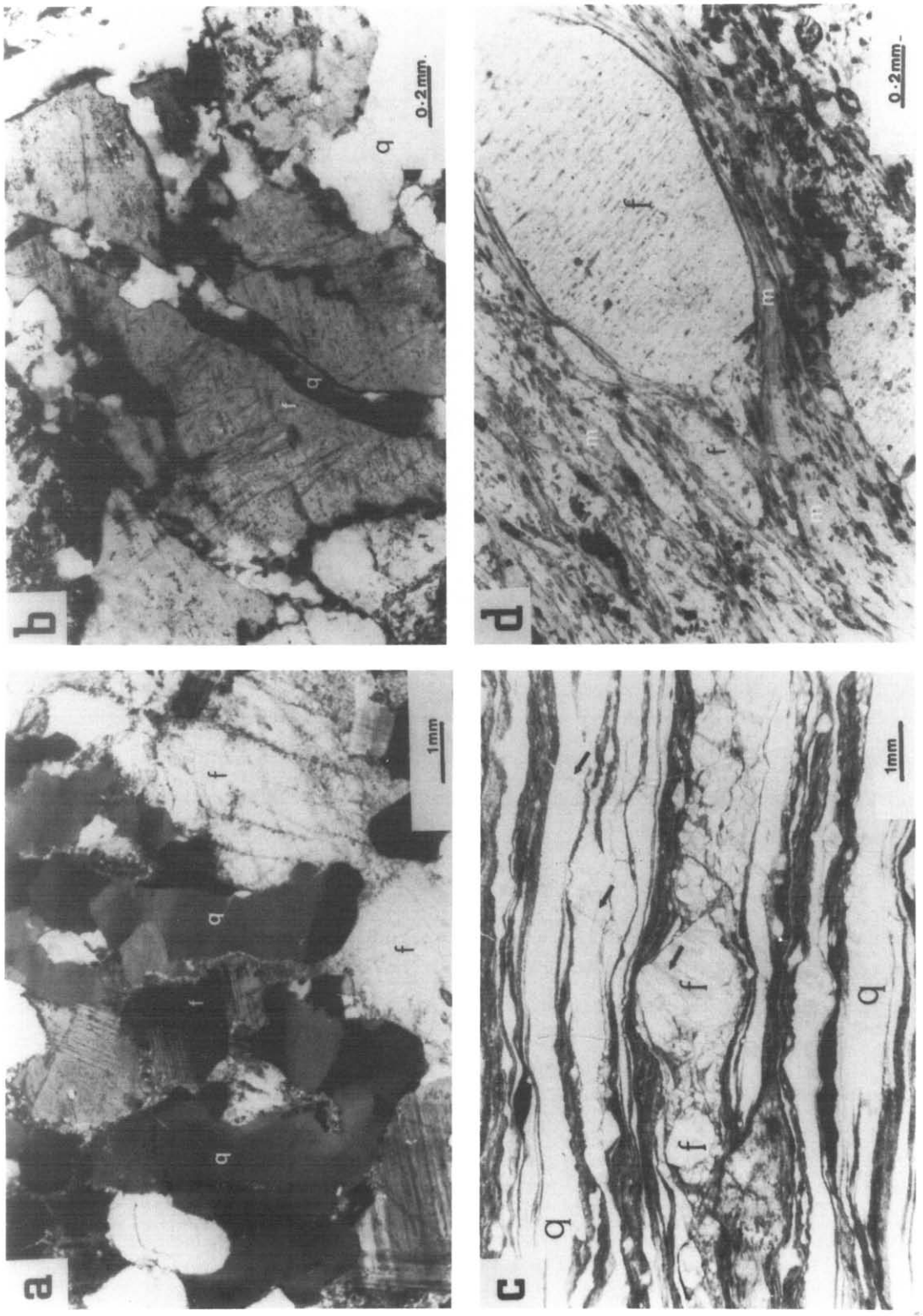

Fig. 2. All sections normal to foliation. (a) Protolith gneiss consisting of quartz (q) showing undulose extinction and alkali feldspar (f) showing incipient alteration to white mica along fractures. Albite-twinned plagioclase appears to be relatively unaltered. Vertical foliation is defined by elongate quartz grains. Open symbols in Fig. 4 indicate the shapes of quartz and feldspar grains in this sample. Crossed polarized light. (b) Cataclastically deformed alkali feldspar (f) in protomylonite displaying angular fragments. Fractures filled with quartz (q). Crossed polarized light. (c) Laminated mylonite showing elongated monocrystalline quartz ribbons (q) surrounding more equant fractured alkali feldspar (f) clasts. Dark laminations consist of fine-grained muscovite, chlorite, quartz and high relief phases such as epidote, zircon, magnetite and apatite. Arrows indicate oblique healed transgranular microfractures. Sample RW-1, Table 3. *XZ* section. Plane polarized light. (d) Mylonitic foliation, defined mainly by muscovite (m) and chlorite, wrapping around oval shaped and flattened perthitic alkali feldspar (f) clasts. Matrix contains concentrations of epidote, zircon, apatite and ilmenite. Plane polarized light.

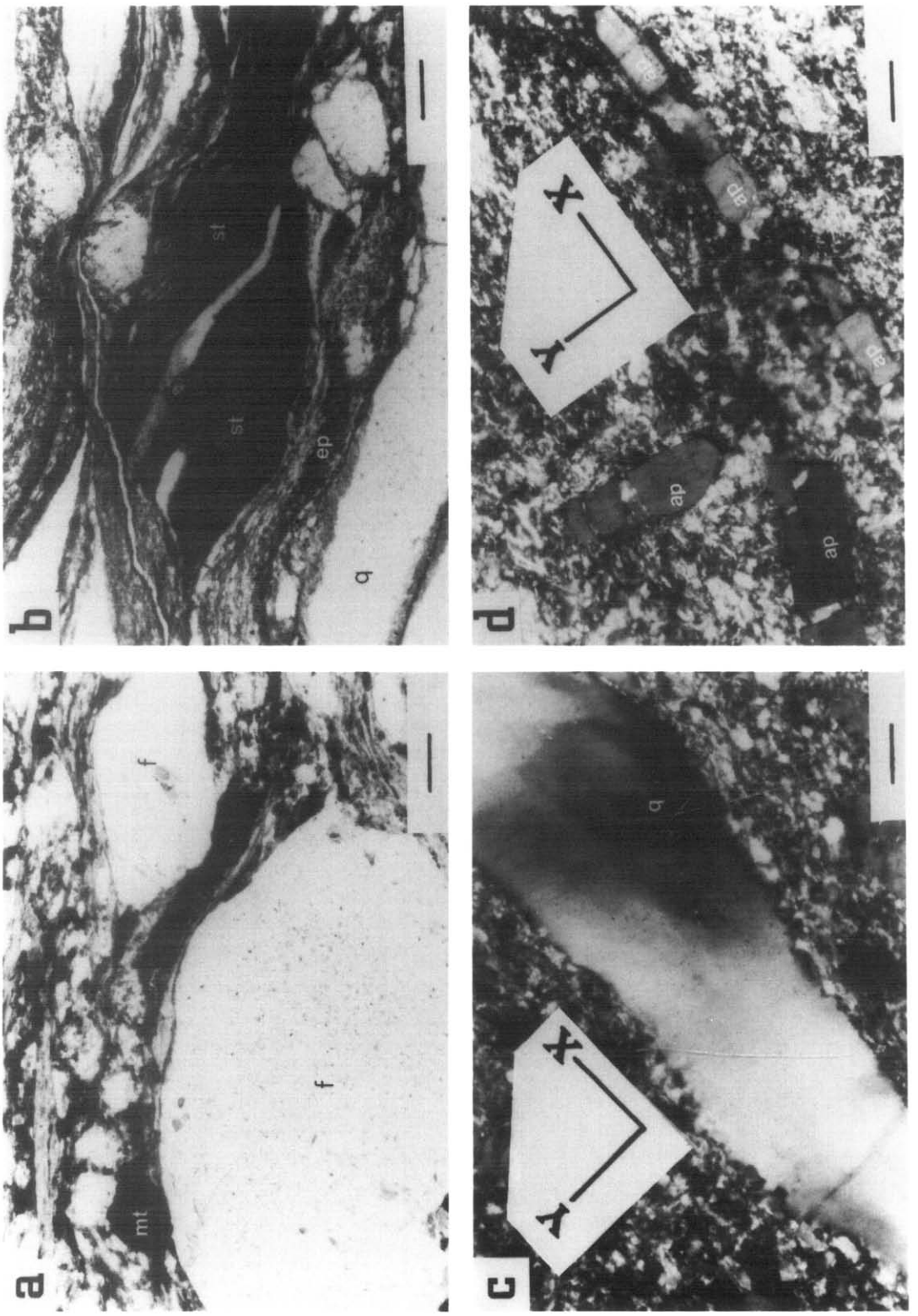

Fig. 3. Sections (a) and (b) are normal to the foliation and sections (c) and (d) are parallel. All scale bars 0.2 mm. (a) Concentrations of refractory phases (e.g. mt, magnetite) along mylonitic foliation surrounding elliptical alkali feldspar clasts (f). Muscovite defines the foliation and is present as selvages around the feldspar grains. Incongruent dissolution of feldspar normal to the foliation is inferred. Trace element enrichments in bulk-rock samples suggest dissolution resulted in volume losses (Figs. 5 and 6). (b) Sheared quartz (q), stilpnomelane (st) and epidote (ep) assemblage indicating greenschist-facies conditions. Tails on stilpnomelane 'mica-fish' indicate left-lateral shear. Plane polarized light. (c) Section parallel to the foliation displaying an undulose quartz grain elongated in the X direction, defining the mylonitic lineation. Sample NC-17, Table 3. Crossed polarized light. (d) Section parallel to the foliation showing apatite (ap) grains parallel, normal and at an intermediate angle to the X direction. The boudinaged grain parallel to X shows maximum extension (110%), whereas the grain parallel to Y shows only minor extension across fractures. This pattern of deformation is consistent with plane strain ($\varepsilon_y = 0$). Same sample as (c).

Table 3. Measured and calculated strain values

	Quartz					Feldspar				
Sample	*Y/Z*	S.D.	*X/Y*	S.D.	*k*	*Y/Z*	S.D.	*X/Y*	S.D.	*k*
VA-4	4.4	1.8	1.7	1.6	0.2	2.2	0.7	1.3	0.7	0.2
NC-17	3.5	0.9	3.3	1.3	0.9					
VA-6						2.5	1.3	1.1	0.2	0.1
NC-17A	2.8	1.0	2.0	0.7	0.6	2.5	0.6	1.2	0.4	0.1
RW-1	12.8	6.9	5.1	2.8	0.3					
NC-19	2.7	1.6	2.4	1.2	0.8	1.0	0.4	1.3	0.1	0.1
NC-1	2.5	1.1	1.0	0.6	0.0	1.6	0.3	1.0	0.2	0.0
NC-16	5.3	2.1	1.9	0.3	0.2					
NC-15	4.4	2.7	3.5	1.1	0.7	1.8	0.4	1.4	0.4	0.5

$k = [(X/Y - 1)/(Y/Z - 1)]$; Flinn (1965).

case of feldspar some shape changes, in addition to pressure solution, were caused by cataclasis. For example, the sample of feldspar from the protolith gneiss probably reflects fracture of feldspar along cleavage planes rather than constrictional strain (open triangle, Fig. 4). These processes reduced the number of valid measurements per sample and together with the heterogeneous nature of the deformation resulted in a relatively large analytical error (Fig. 4).

Secondly, because the protolith gneisses have a regional foliation the final shape of the mineral strain ellipsoid will reflect the superposition of strain of this foliation and the mylonitic fabric. However, except in circumstances where the *XY* plane of the superposed strain is normal to the initial flattening plane and the *X* direction parallel to this plane the resultant total strains will be oblate (Sanderson 1976). The approximate parallelism of the pre-mylonitic and the mylonitic foliation indicates therefore that the observed strain will overestimate the oblate component of the mylonitic fabric and the *k* values indicated will be minimum values. A comparison of the intensity of the pre-mylonitic and mylonitic fabrics (Figs. 2a & c) indicates, however, that this overestimation of the oblate component of strain will not dominate the total strain.

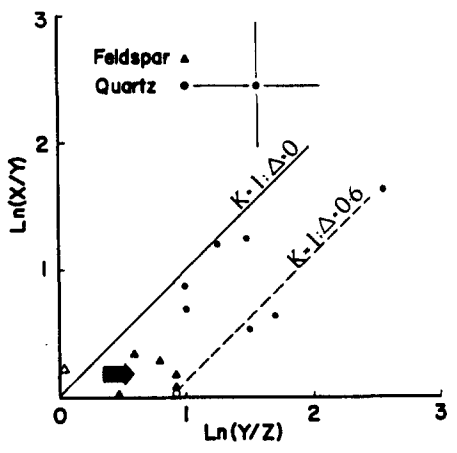

Fig. 4. Logarithmic Flinn diagram showing quartz and feldspar grain shapes based on data in Table 3 for samples from the Fries and Rector Branch Thrusts. Open symbols represent protolith gneiss (Fig. 2a). Dashed line represents plane strain ($k = 1$) at 60% volume loss. The feldspar data are consistent with the interpretation that they obtained their shape in the mylonites by volume loss normal to the foliation (dark arrow), without substantial change in the *X* or *Y* direction. Quartz data show a wide range of *k* values (Table 3). Error bars represent the average standard deviation for quartz.

The data presented so far largely refer to strain on the grain scale, which on account of the contrasting behavior of different minerals, may or may not reflect bulk-rock behavior. In contrast, trace element enrichments in the mylonites, which are interpreted as due to large volume losses (O'Hara & Blackburn 1989), do reflect bulk-rock behavior. The nature and magnitude of this dilational component of strain is addressed below.

VOLUME LOSS

Theoretical relationships

A general relationship between trace element enrichment and finite strain is presented below in the context of fluid–rock interaction. By mass balance the amount of any element in a fluid–rock system is given by:

$$C_i M_i = C_w(M_i - M_f) + C_f M_f, \quad (1)$$

where C_i and C_f refer to initial and final concentrations, and M_i and M_f refer to initial and final masses in the rock, respectively. C_w refers to the concentration in the fluid. If, however, the element in question is assumed to be largely immobile, then C_w will be close to zero. Assuming also density changes are minor (Table 1) equation (1) reduces to:

$$C_i V_i = C_f V_f, \quad (2)$$

where *V* refers to volume. In terms of the more familiar dilation which is defined as:

$$\Delta = (V_f - V_i)/V_i$$

equation (2) can be rewritten as:

$$C_f/C_i = 1/(1 + \Delta) \quad (3)$$

or

$$C_f/C_i = 1/[(1 + e_x)(1 + e_y)(1 + e_z)], \quad (4)$$

where e_x, e_y and e_z are the maximum, intermediate and minimum principal finite elongations, respectively. C_f/C_i is an enrichment factor and graphically it represents the slope of the best-fit line to immobile trace

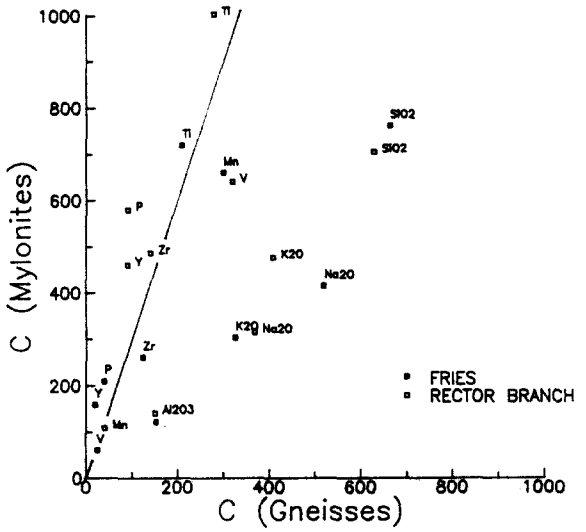

Fig. 5. Plot of average concentration of 'immobile' trace elements (Ti, Zr, P, Y, Mn and V) and selected major elements in protolith gneisses versus average concentration in mylonites from the Fries Thrust (closed squares) and the Rector Branch Thrust (open squares). Based on data in Table 2, arbitrarily scaled to fit on the diagram. The slope of the best-fit line to the trace element data is 3.1 ($r^2 = 0.65$), corresponding to a volume loss of 68% in the average mylonite, assuming these elements were immobile. Major elements below this line are interpreted as mobile (Grant 1985, O'Hara 1988).

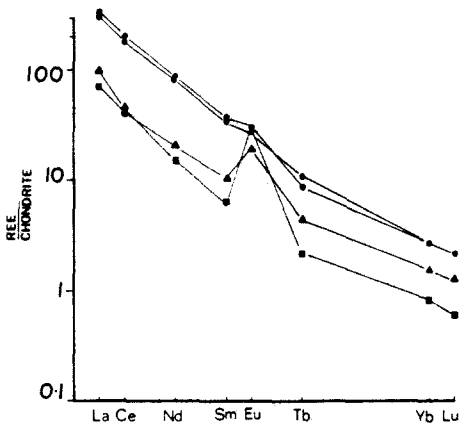

Fig. 6. Chrondrite-normalized rare earth element concentrations (log scale) for gneiss (squares), protomylonite (triangles) and mylonites (circles) for a single outcrop associated with the Rector Branch Thrust. Analyses by neutron activation. Major and minor element chemistry of samples are presented in Table 1 of O'Hara (1988). Note subparallelism of patterns, the approximate three fold enrichment in the mylonites and the smaller positive europium (Eu) anomaly with progressive mylonitization.

element data on a plot of the concentration in the protolith versus the concentration in the mylonites.

Chemical analyses

Whole-rock major and selected trace element analyses of samples of gneisses and mylonites from the Fries Thrust and from the Rector Branch Thrust are summarized in Table 2. Figure 5 is a plot of the average concentration of selected trace and major elements in gneisses versus their concentrations in the mylonites. Within analytical error the mylonites are substantially enriched in Ti, P, Zr, Mn and V (and also in FeO and MgO) relative to the gneisses at both localities. The trace element enrichments are attributed to refractory phases such as zircon (Zr^{4+}, P^{5+}), apatite (P^{5+}), ilmenite (Ti^{4+}) and epidote (Y^{3+}) which are present in the protolith gneisses and conspicuous in the mylonites (e.g. Figs. 2d and 3a). These mineral phases, depending on the chemistry of the fluid phase and the conditions of deformation, may fracture, recrystallize or dissolve (e.g. Wayne & Sinha 1988). Because of the low solubility of the high valence cations (e.g. Ti^{4+}, P^{5+}, Y^{3+}) however, their release during the breakdown of their host phase can be expected to result in local redistribution (e.g. into new overgrowths, Wayne & Sinha 1988) and on the whole-rock scale they can be presumed to be largely immobile. The widespread success in using Ti, Y and Zr concentrations in hydrothermally altered rocks, for example, to identify their primary magmatic signatures supports this conclusion (Pearce & Cann 1973). The trace element enrichments, therefore, are interpreted as due to large volume loss rather than mobility of these elements (O'Hara & Blackburn 1989).

In support of this deduction, the trivalent rare earth elements (REE), commonly regarded as immobile (Hanson 1980), are progressively enriched in protomylonite and mylonite samples compared to the protolith gneiss for a single outcrop from the Rector Branch Thrust (Fig. 6). Modally, feldspar decreases from 40% in the gneiss, to 17% in the protomylonite, to 12% and 11% in the mylonites. Ignoring Eu for the present, their REE patterns are nearly parallel (with the exception of the light rare earths La, Ce and Nd in the protomylonite). This suggests that (1) these rocks are related petrogenetically (i.e. the gneiss is the protolith of the mylonites) and (2) that either substantial fractionation of the REE during mylonitization did not occur (i.e. they were largely immobile) or that both the light and heavy REE fractionated by the same amount and in the same sense (i.e. from fluid to rock) during mylonitization. Since the REE exhibit large and systematic variations in their partitioning behavior from the light to the heavy elements, this latter possibility can be largely discounted. In granitoid rocks the REE reside mainly in accessory phases such as apatite, zircon and epidote (Gromet & Silver 1983). Some suggestion of selective light REE mobility in the protomylonite (Fig. 6) might be attributed to fracturing and dissolution of these host minerals, since cataclasis (in the presence of a fluid) is an important mechanism of grain-size reduction in the protomylonites (e.g. Figs. 2b and 3d).

The approximate three-fold enrichment of REE in the mylonites (Fig. 6) is in agreement with the slope of 3.1 ($r^2 = 0.65$) for the best-fit line to the other trace elements in Fig. 5. These enrichments correspond to a volume loss of 68% using equation (3) above. The substantial scatter about this line may be due to a combination of analytical uncertainty, protolith heterogeneities, variable volume losses, and selective mobility of some elements.

Major elements such as SiO_2, Al_2O_3, Na_2O and K_2O in Fig. 5 plot below the regression line. This is consistent with the interpretation that these elements were lost from the system (Grant 1985). Microstructural (Figs. 2d

and 3a) and modal (Table 1) observations suggest that feldspar dissolution occurred which is also consistent with the release of silica and alkalis to the fluid phase according to the following reactions:

$$\tfrac{3}{2}\text{K-spar} + H^+ = \tfrac{1}{2}\text{Musc.} + 3SiO_2 + K^+$$

or

$$2\text{Albite} + \text{K-spar} + 2H^+ = \text{Musc.} + 6SiO_2 + 2Na^+.$$

Additional geochemical evidence in favor of feldspar dissolution is provided by the REE data. The large positive Eu anomaly displayed by the gneiss decreases during mylonitization (Fig. 6). Since divalent europium (Eu^{2+}) is hosted mainly by feldspar (Hanson 1980) this behavior is consistent with feldspar dissolution and release of Eu to the fluid phase during mylonitization.

INTERPRETATION OF CHEMICAL AND FINITE STRAIN DATA

Chemical data presented above suggest that the deformation involved volume losses of at least 60% and microstructural, modal and trace element evidence suggest that this was accommodated largely by feldspar dissolution in the direction normal to the foliation.

The deformation path for volume loss normal to the mylonitic foliation (*XY* plane) on a Flinn diagram is parallel to the abscissa (arrow, Fig. 4), since X/Y remains constant while Z decreases. The percentage volume loss involved is equal to the percentage shortening in the Z direction (i.e. e_x, $e_y = 0$ and $e_z = -0.6$). This type of deformation plots in the flattening field on a Flinn diagram. It is important to clearly distinguish this apparent flattening strain from true flattening, because the former implies e_x and $e_y = 0$, whereas the latter implies e_x and $e_y > 0$. The deformation path for simple shear ($k = 1$) separates the oblate from the prolate fields and is represented by a line of unit slope which is progressively displaced along the abscissa into the oblate field according to the relation $\ln(1 + \Delta)$ (Ramsay & Wood 1973).

The feldspar data (Fig. 4) are consistent with the interpretation that the feldspars obtained their shape by up to 60% shortening in the Z direction ($e_z = -0.6$; $e_y = 0$; $e_x = 0$), corresponding to 60% volume loss in an open system. It should be noted that the volume losses estimated from feldspar grain shapes are minimum values insofar as grain measurements could obviously only be made on feldspars which were not totally dissolved. Moreover, these estimates are not equivalent to bulk-rock estimates based on whole-rock chemistry since feldspar makes up only a fraction of the protolith (typically 40–50%) (Table 1). Clearly, even total dissolution of feldspar in the protolith could not produce a bulk 60% volume loss, particularly when dissolution products such as muscovite and epidote are considered. An alternative possibility is that quartz also underwent dissolution, though microstructural evidence for this is lacking. Dislocation creep mechanisms may have masked any microstructural evidence for quartz dissolution.

The data for quartz plot in the apparent flattening field below the line $k = 1$ and display a wide range of k values. As indicated above, however, these are minimum values that overestimate the flattening component of finite strain. Microstructural evidence presented above (e.g. Fig. 3d) suggests that $e_y = 0$ for some samples, indicating plane strain (i.e. $k = 1$), and asymmetric kinematic indicators (e.g. Fig. 3b) suggest that the deformation was non-coaxial. Although the analytical error on these data is large (Fig. 4), they are consistent with a component of simple shear at least for some of the samples analysed. On the other hand, if quartz deformed in plane strain and also underwent dissolution, as suggested above, then it might be expected that some samples would plot close to a line of unit slope ($k = 1$) that is displaced along the abscissa (e.g. dashed line, Fig. 4). This pattern is observed for three mylonitic samples. If this interpretation is correct estimates of volume loss for individual samples, based on trace element enrichments, should show an inverse correlation with k values. For example, samples close to isovolumetric plane strain should display no trace element enrichments and k values close to one whereas samples close to the 60% volume-loss plane strain line should show a 2.5-fold enrichment and k values less than 1. No correlation between k values and enrichment factors, however, was observed. The variation in k values in quartz apparently reflects the heterogeneous nature of the deformation, which ranges from approximately simple shear to non-coaxial flattening.

In summary, the combined microstructural, trace element and mineral shape fabric data are consistent with a component of heterogeneous shortening normal to the foliation and a component of shear parallel to the foliation. The deformation was partitioned between solution transfer in feldspar and dislocation creep processes in quartz and micas. Bell & Cuff (1989) advocate a similar model involving partitioning of deformation in metamorphic rocks between progressive shortening and shearing components. In the shear band terminology of Cobbold (1977) the mylonites can be described as SP^- structures, where S designates the non-coaxial shear component and P^- indicates shortening normal to the shear plane involving volume loss. Boyer & Mitra (1988) in a study of mylonite zones from the western Blue Ridge province suggested that ductile deformation zones close to major thrusts deformed approximately by simple shear, but that deformation away from thrusts involved bulk heterogeneous coaxial shortening along conjugate shear zones. The similarity of the microstructures in these mylonites to those described here suggests that volume loss may also have been important in some of the zones discussed by Boyer & Mitra (1988).

DISCUSSION

Possibly because of the emphasis in recent years on the importance of crystal-plastic mechanisms in mylo-

nites, processes that are essentially isovolumetric, the role of volume loss in mylonite petrogenesis has received less attention. Unless volume changes are known, however, the flow pattern in ductile shear zones is poorly constrained (e.g. Mawer 1983) and a variety of strain histories are permissible. For example, volume loss relaxes constraints which restrict flow in ideal (i.e. parallel sided, rigid walled) shear zones to simple shearing (Ramsay & Graham 1970). Similarly, strain compatibility constraints associated with bulk shortening (Bell 1981), a deformation pattern which appears to be important in some crystalline terranes (Choukroune & Gapais 1983, Boyer & Mitra 1988) are also relaxed when volume change is permitted. This is important because bulk shortening without volume loss results in crustal thickening (Bell 1981) which in orogenic belts has several important geologic consequences. Lastly, as pointed out by Ramsay & Huber (1987, p. 610), strain compatibility can only occur in the shear band model of Cobbold (1977) if volume loss is involved.

Strain estimates in shear zones will also be in error unless volume change is recognized. For example, displacements based on integrated shear strain techniques across what otherwise appear to be ideal shear zones will result (in the case of volume loss) in overestimates (Coward & Potts 1983), and apparent flattening finite strains in such zones may also be incorrectly attributed to true flattening unless volume loss is taken into account. Although many of these aspects of volume loss have been known for some time (e.g. Ramsay & Graham 1970, Ramsay & Wood 1973) the difficulty in measuring volume changes during deformation in many structural studies has led to the common assumption of isovolumetric behavior. Some of the difficulty in recognizing volume loss arises from the fact that chemical analyses are normally summed to 100% and if elements are removed during deformation in proportion to their initial abundance, then the percentage concentration in the altered rock will appear substantially unchanged in comparison to the protolith.

Because strain in the continental crust is heterogeneously distributed the nucleation and growth of high strain zones is important to understanding crustal behavior. A fundamental finding of fracture mechanics is that shear fractures (Mode II) cannot propagate in their own plane (e.g. Scholz 1989) thereby creating a problem for the origin and propagation of faults and shear zones in general. In some cases it has been shown that ductile shear zones nucleated on pre-existing joints (Segall & Simpson 1986). In the case of ductile shear zones of the type described here it is suggested that they may nucleate on pre-existing solution zones. The process of solution transfer is thought to produce stress concentrations in the surrounding rock which results in propagation of the solution zone (or 'anticrack') in a manner similar to a tensile crack (Fletcher & Pollard 1981). The early stages of formation of solution zones in granite have been described by Burg & Iglesias Ponce de Leon (1985). Similar zones could accommodate displacement parallel to the zone boundaries, particularly if strain softening occurred as a result of feldspar dissolution and growth of phyllosilicates (O'Hara 1988). Thus, ductile shear zones of the type described here may nucleate along pre-existing solution zones in crystalline rocks and subsequently become reactivated as shear zones under suitable stress conditions. The transition from bulk coaxial shortening to dominantly simple shear observed by Boyer & Mitra (1988) in the crystalline gneisses of the western Blue Ridge province might reflect such a process.

In terms of deformation mechanisms, the progressive shearing and shortening components of deformation observed in this study are thought to be related. Review of experimental evidence of silicate dissolution indicates that the rate of dissolution at fixed temperature and pH is controlled by the effective surface area (Wood & Walther 1983). Insofar as grain-size reduction of feldspars by cataclasis during progressive shearing increases surface area, dissolution will be facilitated. Similarly, unless shearing along the margins of feldspars exposed a new surface to the surrounding fluid, armoring of feldspar by reaction products such as muscovite would occur and dissolution would cease. Therefore progressive shearing will enhance the dissolution process and the two processes are inferred to operate in concert. If shearing caused cataclastic or plastic damage to the margins of feldspar grains then these areas might be expected to undergo preferential dissolution (Wintsch & Dunning 1985). In this case the dissolution process would be distinct from pressure solution which is only weakly dependent on temperature but depends largely on the magnitude of the differential stress (Rutter 1983).

Some insight into the process of feldspar dissolution and consequent volume loss may be gained by examining the analogous but better understood surface weathering process of saprolite production. In saprolite, mass is lost during replacement of feldspars by clays while volume is preserved (Velbel 1988). Density therefore is considerably lowered, typically from 2.8 to 1.6 g cm^{-3} and the porosity increases to approximately 40%. The increased porosity facilitates fluid infiltration leading to further saprolite production and the resulting metasomatic changes include losses of silica and alkalis (Velbel 1988). During mylonitization similar processes are inferred to operate, except that as dissolution proceeds, fluid-filled pore spaces will close, depending on the fluid pressure. The relationship of pore collapse to pore creation will control the permeability of the rock and will depend on, among other variables, the effective stress (Brace 1972), displacement history (Makurat 1985) and the dissolution rate (Etheridge *et al.* 1984, p. 4354). Because shortening normal to the foliation in the mylonites is accommodated largely by dissolution, the strain rate in this direction ($\dot{e}_z$) will correspond to the rate of dissolution, assuming solute removal is sufficiently rapid. At 400°C, the approximate conditions of mylonitization (see above), the silicate dissolution rate is 5×10^{-12} mol cm^{-2} s^{-1} (equation 5 of Wood & Walther 1983), corresponding to a strain rate ($\dot{e}_z$) of 5×10^{-12} s^{-1}. If progressive shearing is the rate limiting process

for dissolution then this would represent a maximum value.

Elevated fluid pressure would inhibit collapse of voids created during dissolution thereby substantially increasing the permeability of the rock (Brace 1972). Also experimental studies indicate that shearing increases the permeability along sliding surfaces by several orders of magnitude (Makurat 1985). Under these circumstances sheared asperities would likely undergo rapid dissolution rather than contributing to a gouge layer. In addition, fluid flow in a direction of increased temperature (possibly upward in a thrust setting) would also enhance the permeability through dissolution (Morrow *et al.* 1981). On the other hand, quartz plasticity might be expected to inhibit the development of an interconnected porosity. Fluid pathways under these dynamic conditions can be expected to be temporally and spatially complex and leave little record of their nature, except for concentrations of residual minerals (e.g. zircon, epidote and apatite) and reaction products (e.g. muscovite, epidote and chlorite). The large volume losses indicated and the large fluid–rock volume ratios they imply (10^2–10^3, O'Hara & Blackburn 1989) are nevertheless testament to the prior existence of extensive, though perhaps short-lived, high permeability zones in these rocks.

CONCLUSIONS

(1) Deformation in the mylonites was partitioned between solution transfer and crystal-plastic mechanisms at temperatures between approximately 300 and 450°C.

(2) Flattened alkali feldspar grain shapes are largely the result of dissolution normal to the foliation. Progressive shearing parallel to the foliation probably facilitated the dissolution process.

(3) Quartz deformed heterogeneously by dislocation creep processes and involved a combination of simple shear and non-coaxial flattening.

(4) Three-fold enrichment in 'immobile' trace elements, including the rare earth elements, is interpreted as due to >60% bulk volume loss in the mylonites. Volume loss was accommodated by dissolution of feldspar (and possibly quartz) and resulted in the accumulation of residual accessory phases in the mylonites and loss of silica and alkalis to the fluid phase.

Acknowledgements—Careful reviews by Chris Mawer and an anonymous reviewer substantially improved the manuscript and are gratefully acknowledged. Nick Rast suggested improvements in the final version of the text. The author however takes responsibility for any errors in fact or interpretation. This research was supported by a grant from the Petroleum Research Fund, administered by the American Chemical Society.

REFERENCES

Bell, T. H. 1981. Foliation development—the contribution, geometry and significance of progressive, bulk, inhomogeneous shortening. *Tectonophysics* **75**, 273–296.

Bell, T. H. & Cuff, C. 1989. Dissolution, solution transfer, diffusion versus fluid flow and volume loss during deformation/metamorphism. *J. metamorph. Geol.* **7**, 425–447.

Berthé, D., Choukroune, P. & Jegouzo, P. 1979. Orthogneiss, mylonite and non coaxial deformation of granites: the example of the South Armorican shear zone. *J. Struct. Geol.* **1**, 31–42.

Boyer, S. E. & Mitra, G. 1988. Relations between deformation of crystalline basement and sedimentary cover at the basement/cover transition zone of the Appalachian Blue Ridge Province. In: *Geometries and Mechanisms of Thrusting, with Special Reference to the Appalachians* (edited by Mitra, G. & Wojtal, S.). *Spec. Publ. geol. Soc. Am.* **222**, 119–136.

Brace, W. F. 1972. Pore pressure in geophysics. In: *Flow and Fracture of Rocks—Griggs Volume* (edited by Spilhaus, A. F.). *Am. Geophys. Un. Geophys. Monogr.* **16**, 265–273.

Burg, J. P. & Iglesias Ponce de Leon, M. 1985. Pressure-solution structures in a granite. *J. Struct. Geol.* **7**, 431–436.

Choukroune, P. & Gapais, D. 1983. Strain pattern in the Aar Granite (Central Alps): orthogneiss developed by bulk inhomogeneous flattening. *J. Struct. Geol.* **5**, 412–418.

Cobbold, P. R. 1977. Description and origin of banded deformation structures. I. Regional strain, local perturbations and deformation bands. *Can. J. Earth Sci.* **14**, 1721–1731.

Coward, M. P. 1976. Strain within ductile shear zones. *Tectonophysics* **34**, 181–197.

Coward, M. P. & Potts, G. J. 1983. Complex strain patterns developed at the frontal and lateral tips to shear zones and thrust zones. *J. Struct. Geol.* **5**, 383–399.

Escher, A., Escher, J. C. & Waterson, J. 1975. The reorientation of the Kangamiut dike swarm, West Greenland. *Can. J. Earth Sci.* **12**, 158–173.

Etheridge, M. A., Wall, V. J. & Cox, S. F. 1984. High fluid pressures during regional metamorphism and deformation: implications for mass transport and deformation mechanisms. *J. geophys. Res.* **89**, 4344–4358.

Fletcher, R. C. & Pollard, D. D. 1981. Anticrack model for pressure solution surfaces. *Geology* **9**, 419–424.

Flinn, D. 1965. On the symmetry principle and the deformation ellipsoid. *Geol. Mag.* **102**, 36–45.

Grant, J. A. 1985. The isocon diagram—a simple solution to Gresens equation for metasomatic alteration. *Econ. Geol.* **81**, 1976–1982.

Gromet, L. P. & Silver, L. T. 1983. Rare earth elements among minerals in a granodiorite and their petrogenetic implications. *Geochim. cosmochim. Acta* **47**, 925–939.

Hanson, G. N. 1980. Rare earth elements in petrogenetic studies of igneous systems. *Annu. Rev. Earth & Planet. Sci.* **8**, 371–406.

Janecke, S. U. & Evans, J. P. 1988. Feldspar-influenced rock rheologies. *Geology* **16**, 1064–1067.

Makurat, A. 1985. The effect of shear displacement on the permeability of natural rough joints. *Proc. 17th Congr. Ass. Hydrogeol.*, Tucson, 99–106.

Mawer, C. K. 1983. State of strain in a quartzite mylonite, Central Australia. *J. Struct. Geol.* **5**, 401–409.

Mitra, G. 1978. Ductile deformation zones and mylonites: the mechanical processes involved in the deformation of crystalline basement rocks. *Am. J. Sci.* **278**, 1057–1084.

Morrow, C., Lockner, D., Moore, D. & Byerlee, J. 1981. Permeability of granite in a temperature gradient. *J. geophys. Res.* **86**, 3002–3008.

O'Hara, K. 1988. Fluid flow and volume loss during mylonitization—an origin for phyllonite in an overthrust setting, North Carolina, U.S.A. *Tectonophysics* **156**, 21–36.

O'Hara, K. & Blackburn, W. H. 1989. Volume-loss model for trace element enrichments in mylonites. *Geology* **17**, 524–527.

Oriel, S. S. 1951. Structure of the Hot Springs window, Madison County, North Carolina. *Am. J. Sci.* **249**, 1–30.

Passchier, C. W. & Simpson, C. 1986. Porphyroclast systems as kinematic indicators. *J. Struct. Geol.* **8**, 831–843.

Pearce, J. S. & Cann, J. R. 1973. Tectonic setting of basic volcanic rocks determined using trace element analysis. *Earth Planet. Sci. Lett.* **19**, 290–300.

Ramsay, J. G. & Graham, R. H. 1970. Strain variation in shear belts. *Can. J. Earth Sci.* **7**, 786–813.

Ramsay, J. G. & Huber, M. I. 1987. *The Techniques of Modern Structural Geology, Volume* 2: *Folds and Fractures*. Academic Press, New York, 309–700.

Ramsay J. G. & Wood, D. S. 1973. The geometric effects of volume change during deformation processes. *Tectonophysics* **16**, 263–277.

Rutter, E. H. 1983. Pressure solution in nature, theory and experiment. *J. geol. Soc. Lond.* **140**, 725–740.

Sanderson, D. J. 1976. The superposition of compaction and plane strain. *Tectonophysics* **30**, 35–54.
Segall, P. & Simpson, C. 1986. Nucleation of ductile shear zones on dilatant fractures. *Geology* **14**, 56–59.
Scholz, C. H. 1989. Mechanics of faulting. *Annu. Rev. Earth & Planet. Sci.* **17**, 309–334.
Simpson, C. 1983. Strain and shape-fabric variations associated with ductile shear zones. *J. Struct. Geol.* **5**, 61–72.
Stose, A. J. & Stose, G. W. 1957. Geology and mineral resources of the Gossan Lead district and adjacent areas in Virginia. *Bull. Virginia Div. Miner. Resour.* **72**, 134.
Tullis, J. 1983. Deformation in feldspars. In: *Feldspar Mineralogy, Volume* 2 (edited by Ribbe, H. P.). *Miner. Soc. Am.*, 297–323.
Velbel, M. A. 1988. Weathering and soil-forming processes. In: *Ecological Studies, 66, Forest Hydrology and Ecology at Coweeta* (edited by Swank, W. T. & Crossbey, D. A.). Springer, New York, 91–102.
Voll, G. 1976. Recrystallization of quartz, biotite and feldspars from the Erstfeld to the Leventina nappe, Swiss Alps, and its geological significance. *Schweiz. miner. petrogr. Mitt.* **56**, 641–647.
Wayne, D. M. & Sinha, A. K. 1988. Physical and chemical response of zircon to deformation. *Contr. Miner. Petrol.* **98**, 109–121.
Winkler, H. G. F. 1974. *Petrogenesis of Metamorphic Rocks* (4th edn). Springer, New York.
Wintsch, R. P. & Dunning, J. 1985. The effects of dislocation density on the aqueous solubility of quartz and some geologic implications: a theoretical approach. *J. geophys. Res.* **90**, 3649–3657.
Wood, B. J. & Walther, J. V. 1983. Rates of hydrothermal alteration. *Science* **222**, 413–415.